Acta Cryst. (1984). B40, 14–20

Room- and High-Pressure Crystal Chemistry of CoAs and FeAs

BY PETER S. LYMAN* AND CHARLES T. PREWITT

Department of Earth and Space Sciences, State University of New York, Stony Brook, New York 11794, *USA*

(*Received* 1 *January* 1983; *accepted* 1 *September* 1983)

Abstract

The MnP-type crystal structures of FeAs and CoAs have been studied at both room and high pressure. In the room-pressure study, refinements of both structures were carried out in space groups *Pnam* and $Pna2_1$ using single-crystal integrated X-ray intensity data collected from a four-circle diffractometer. For CoAs, both space groups refined to a weighted residual, $R_w = 0{\cdot}054$, whereas for FeAs, $R_w = 0{\cdot}030$ for *Pnam* and 0·027 for $Pna2_1$. The Hamilton significance test, applied to FeAs, shows a significant improvement in R_w for $Pna2_1$. However, the Hamilton test is not a conclusive test for space-group identity. Comparison of interatomic distances, derived from *Pnam* and $Pna2_1$ refinements for both CoAs and FeAs, shows no significant change in the structures. High-pressure X-ray data were collected from single crystals enclosed in a Merrill & Bassett-type diamond-anvil cell. Cell parameters and structures were refined at 2·80 (5), 3·70 (5), and 4·90 (5) GPa for CoAs, and at 2·25 (5), 4·36 (5), 6·10 (5), and 8·3 (3) GPa for FeAs. Cell data were used to determine the elastic constants, isothermal bulk modulus and its pressure derivative (K_T and K'_T, respectively), by least-squares fitting of the unit-cell volumes to a third-order Birch–Murnaghan equation of state. This gave $K_T = 123$ (6) GPa and $K'_T = 8{\cdot}8(3{\cdot}3)$ for CoAs. For FeAs, $K_T = 118$ (4) GPa and $K'_T = 7{\cdot}2$ (1·8). Refinements in *Pnam* show that the structure remains an MnP-type throughout these pressure ranges. A precession photograph of CoAs at 7·8 GPa revealed previously sharp split and diffuse diffraction spots. Similar effects are known to occur in FeS when it undergoes a change from an MnP-type structure to a high-pressure phase above 6·8 GPa. Thus, these effects in CoAs may indicate the onset of a phase transition. Changes in both interatomic distances and atomic displacements from positions in an NiAs-type structure reveal some interesting aspects of the anisotropic compression these compounds undergo. These changes are correlated with high-pressure phase transitions that may occur in MnP-type structures.

Introduction

At ambient conditions, CoAs and FeAs are two of about 30 compounds that take the MnP-type structure, a structure related to the hexagonal NiAs-type structure by a small distortion. Although the structures of MnP-type compounds are well known, there exists ambiguity in space-group assignment centered around the presence or absence of mirror symmetry. Because most of the previous studies involved film techniques, we report below the results of single-crystal X-ray diffraction experiments on CoAs and FeAs using data collected with a four-circle diffractometer.

A recent high-pressure structural study of FeS (King, 1979; King & Prewitt, 1982), which has an MnP-type structure above 3·4 GPa, revealed a transition at 6·7 GPa. However, experimental difficulties prevented characterization of the high-pressure phase. It is reasonable to expect that other MnP-type compounds may undergo an analogous phase transition. Thus, we have undertaken a high-pressure structural study of CoAs and FeAs to see: (1) if any phase transitions can be induced, and (2) if their structural behavior is related to that of FeS at high pressure.

Previous work

Fylking (1935) reported solution of structures of the isostructural phases MnP, FeP, CoP, MnAs, FeAs and CoAs, and hence designated MnP as the prototype structure. In performing the first high-temperature study of MnP-type compounds, Heyding & Calvert (1957) discovered that CoAs transforms to an NiAs-type structure at about 1225 K, whereas FeAs approaches this structure as it nears melting [1343(20) K, Selte, Kjekshus & Andresen, 1972]. As part of a major investigation of MnP-type compounds, Selte & Kjekshus (1969) determined accurate structural parameters for FeAs from three-dimensional single-crystal X-ray data, using the multiple-film technique with an integrated Weissenberg camera. Based on results from the Hamilton (1965) significance test, they concluded that $Pna2_1$ was the correct space group. All previous investigators had assumed *Pnam* was correct. Selte & Kjekshus (1973*a*) redetermined the structure of FeAs using data collected from a four-circle diffractometer. The

* Present address: Raytheon Company, Research Division, 131 Spring Street, Lexington, Massachusetts 02173, USA.

0108-7681/84/010014-07$01.50

Hamilton test again suggested $Pna2_1$ to be the correct space group. However, based on the insignificant deviation of z_{As} from 1/4 in $Pna2_1$, they concluded that *Pnam* was correct.

King & Prewitt (1982) studied the room-pressure/high-temperature and room-temperature/high-pressure phase relations of FeS. At ambient conditions FeS has the troilite structure ($P\bar{6}2c$), and is an antiferromagnetic semiconductor. At 470 K FeS undergoes a first-order transition to a triply twinned MnP-type structure (*Pnam*), accompanied by an increase in electrical conductivity. At the Néel temperature ($T_N = 598$ K), FeS undergoes a second-order transition to an NiAs-type structure ($P6_3/mmc$). High-pressure studies showed that at 3·4 GPa FeS again transforms to a triply twinned MnP-type structure with concomitant increase in electrical conductivity. ^{57}Fe Mössbauer studies (King, Virgo & Mao, 1978) also revealed a decrease in magnetic exchange interaction. This phase is stable up to 6·75 GPa whereupon a transition to a high-pressure phase (h.p.p.) occurs with a 9% decrease in volume. This transition is accompanied by complete loss of magnetic ordering. Increased diffuseness, and in some instances splitting of broadened reflection profiles, made structural characterization of FeS (h.p.p.) impossible. Evidence from both Mössbauer spectra and increased electrical conductivity (King, 1979) suggest there is delocalization of a *d* electron above this transition. Based on similar Mössbauer parameters for FeS (h.p.p.) and (Fe, Co)S, McCammon (1982) proposed that the behavior of FeS (h.p.p.) may be similar to that of (Fe, Co) S, while indicating this can only be tested after structural characterization of FeS (h.p.p.) is complete.

Experimental

Synthesis

Preparation of single crystals of CoAs and FeAs followed the technique described by Selte & Kjekshus (1971). The starting materials were 99·9% pure, 325 mesh metal (Fe or Co) powder and 99·9% pure arsenic pieces. Arsenic was added first to silica tubes. Addition of a slight excess (~0·05%) of reduced metal ensured complete reaction of the arsenic. The vacuum-sealed charges, of approximately 1000–1500 mg, were heated slowly to 1173 K over a 24 h period. They soaked for four days before being cooled slowly to 673 K. For FeAs the polycrystalline product contained some single crystals large enough (0·10 mm) for X-ray work. More single crystals were obtained by re-annealing for seven days before cooling slowly to room temperature over 24 h. To obtain large enough single crystals (>0·20 mm) of CoAs, the chemical vapor transport technique, with iodine as transport agent, was used. Silica tubes with I_2 added as 1 mg per ml of tube volume were sealed under vacuum to a length of approximately 200 mm. They were placed in a horizontal triple-zone furnace with the sample end in the middle zone maintained at 1173 K, while the outer zones were kept at 773–823 K. After one week crystals were distributed throughout the length of the tube. Because many crystals were large (>0·3 mm) and multiply twinned, a steeper gradient was used to promote smaller crystal growth.

Room-pressure measurements

Unit-cell and integrated intensity data were collected from single crystals using a Picker four-circle diffractometer with graphite-monochromatized Mo $K\alpha$ radiation at 50 kV and 14 mA. To ensure that a crystal was properly centered, the diffracted-beam centering technique developed by King & Finger (1979) was used. It has the added feature of providing a very accurate least-squares refinement of the unit-cell parameters. Integrated intensity data were collected in the bisecting position by θ–2θ scans. The constant-precision mode was used in which the scan and background times were adjusted to give a fixed σ_I/I (Finger, Hadidiacos & Ohashi, 1973), within the restriction of a maximum time per reflection. A standard reflection of high intensity was collected at fixed intervals throughout the data collection and only reflections satisfying the condition $3 < 2\theta < 70°$ were collected. Application of a crystal absorption correction to all data sets followed a modified version of Burnham's (1966) program. Input to the program consisted of the absorption coefficient calculated from Hubbell, McMaster, Del Grande & Mallett (1974), and a geometrical model of the crystal relative to the coordinate system of the diffractometer. Data were also corrected for Lorentz and polarization effects.

High-pressure measurements

High-pressure integrated-intensity data were collected in a similar manner as described above except for a few adjustments. Using the techniques of Finger & King (1978), each crystal was mounted in a Merrill & Bassett (1974)-type diamond-anvil cell. A 4:1 methanol–ethanol mixture was used as the hydrostatic pressure medium (Piermarini, Block & Barnett, 1973). Pressures were calibrated through wavelength measurements of the R_1 line from a small (<30 μm) Cr-doped ruby chip that was placed within the sample chamber (Barnett, Block & Piermarini, 1973; Piermarini, Block, Barnett & Forman, 1975). The pressure uncertainty was 0·05 GPa (King & Prewitt, 1980). Integrated-intensity data were collected in the fixed-φ mode (Finger & King, 1978) which allows the maximum amount of data to be collected. Data collected outside the solid angle ($\psi = 42°$) of the diamond-anvil cell were rejected. For CoAs, data were not

collected on reflections whose 2θ values overlapped any of the four most intense beryllium powder rings. However, for FeAs all data within the 2θ limits were collected. Thus, all high-pressure FeAs data were checked for both anomalously high background and incompatibility of symmetrically equivalent reflections. In addition to the crystal absorption correction, high-pressure data also required a correction for absorption by the diamond-anvil cell. The method of Finger & King (1978) calculates this empirically.

Structure refinement

Least-squares refinements of all data were carried out with the program *RFINE4* (Finger & Prince, 1975). This program minimizes the function $\sum w(|F_o|-|F_c|)^2$, where w, the weight for each reflection, was set equal to $1/\sigma_F^2$. All data, including those with $I<2\sigma_I$, were used in the refinements. The final cycles of refinement used data averaged according to orthorhombic symmetry. All refinements used scattering factors for neutral atoms including correction for anomalous dispersion (Cromer & Waber, 1974).*

Results and discussion

Room-pressure studies

Preliminary study using precession photography confirmed the diffraction symbol to be *mmmPna*– for both CoAs and FeAs. Thus *Pnam* and $Pna2_1$ are the only possible space groups. CoAs room-pressure data were collected on a small ($0{\cdot}07\times0{\cdot}09\times0{\cdot}13$mm) single crystal mounted on a glass fiber and standard goniometer head. Least-squares refinement of the unit-cell parameters gave the values $a=5{\cdot}2857\,(6)$, $b=5{\cdot}8675\,(6)$ and $c=3{\cdot}4883\,(7)$ Å. These are in excellent agreement with results of Selte & Kjekshus (1971), where $a=5{\cdot}2867\,(11)$, $b=5{\cdot}8682\,(14)$ and $c=3{\cdot}4892\,(8)$ Å. Based on this we believe the sample is stoichiometric. A data set of 991 reflections, representing a half-sphere, was reduced to a set of 283 symmetry-independent reflections by averaging according to orthorhombic symmetry. Because they were thought to suffer from severe secondary extinction effects, the four strongest reflections were rejected. Both models yielded a weighted residual, R_w, of 0·054, and an unweighted residual, R, of 0·049. Since the inclusion of five extra parameters did not improve the R factor (Hamilton, 1965), *Pnam* is accepted as the true space group. This is consistent with the requirement that *Pnam* be the space group because of a second-order transition to the NiAs structure at high temperature (Franzen, Haas & Jellinek, 1974). Comparison of the refined parameters (Table 1) shows a difference, though small, only for the z positional parameter. No significant changes in bond distances occur between models (Table 2).

Table 1. *Refined positional parameters for* CoAs *and* FeAs *at room pressure in both Pnam and* $Pna2_1$

Compound	CoAs	CoAs	FeAs	FeAs
Space group	*Pnam*	$Pna2_1$	*Pnam*	$Pna2_1$
	Co[4(*c*)]	Co[4(*a*)]	Fe[4(*c*)]	Fe[4(*a*)]
x	0·0020 (2)	0·0020 (2)	0·0033 (1)	0·00316 (8)
y	0·2002 (2)	0·2003 (2)	0·1993 (1)	0·19929 (7)
z	1/4	1/4	1/4	1/4
	As[(4*c*)]	As[(4*a*)]	As[(4(*c*)]	As[4(*a*)]
x	0·1996 (1)	0·1996 (1)	0·1992 (1)	0·19923 (6)
y	0·5867 (1)	0·5867 (1)	0·5773 (1)	0·57736 (4)
z	1/4	0·2506 (2)	1/4	0·2512 (4)

Table 2. *Nearest-neighbor interatomic distances for* CoAs *and* FeAs *at room pressure in both Pnam and* $Pna2_1$

Compound	CoAs		FeAs	
Space group	*Pnam*	$Pna2_1$	*Pnam*	$Pna2_1$
M–As (Å)	2·322 (1)	2·322 (2)	2·348 (1)	2·348 (1)
	2·444 (1)	2·449 (1)	2·449 (1)	2·453 (2)
	2·444 (1)	2·441 (1)	2·449 (1)	2·447 (2)
	2·396 (1)	2·400 (1)	2·422 (1)	2·425 (2)
	2·396 (1)	2·392 (1)	2·422 (1)	2·419 (2)
	2·497 (1)	2·497 (2)	2·515 (1)	2·515 (1)
M–M (Å)				
Face sharing	2·707 (2)	2·707 (2)	2·788 (1)	2·788 (1)
Edge sharing	2·927 (2)	2·927 (2)	2·935 (1)	2·935 (2)
Edge sharing	3·489 (1)	3·489 (1)	3·371 (1)	3·371 (1)
Edge sharing	3·927 (2)	3·927 (3)	3·997 (2)	3·997 (2)
As–As (Å)	2·922 (1)	2·922 (1)	2·900 (1)	2·900 (1)
	3·265 (1)	3·265 (1)	3·425 (1)	3·425 (1)
	3·489 (1)	3·489 (1)	3·371 (1)	3·371 (1)
	3·455 (1)	3·455 (1)	3·496 (1)	3·496 (1)
	3·764 (1)	3·764 (1)	3·797 (1)	3·797 (1)

Room-pressure data for FeAs were collected (excluding absences) on a small ($0{\cdot}07\times0{\cdot}08\times0{\cdot}12$ mm) crystal. Least-squares refinement of the unit-cell parameters gave $a=5{\cdot}4401\,(5)$, $b=6{\cdot}0259\,(5)$ and $c=3{\cdot}3712\,(4)$ Å. Because these are in excellent agreement with results of Selte & Kjekshus (1973*b*), where $a=5{\cdot}4420\,(7)$, $b=6{\cdot}0278\,(7)$ and $c=3{\cdot}3727\,(6)$ Å, the sample is believed to be stoichiometeric. 528 reflections, representing a 1/4 sphere, were reduced to a set of 276 symmetry-independent reflections. Starting positional parameters were those of Selte & Kjekshus (1973*b*). Final refinement in *Pnam* gave $R_w=0{\cdot}030$ and $R=0{\cdot}023$, whereas that in $Pna2_1$ gave $R_w=0{\cdot}027$ and $R=0{\cdot}021$. As reported by Selte & Kjekshus (1973*b*), results of the Hamilton significance test show a significant improvement in R_w at the 0·05 confidence level. However, comparison of both the refined parameters (Table 1) and the interatomic distances (Table 2) for

* Lists of structure factors and anisotropic thermal parameters have been deposited with the British Library Lending Division as Supplementary Publication No. SUP 38825 (12pp.). Copies may be obtained through The Executive Secretary, International Union of Crystallography, 5 Abbey Square, Chester CH1 2HU, England.

Table 3. *Unit-cell parameters for* CoAs *and* FeAs

	Pressure (GPa)	a (Å)	b (Å)	c (Å)	V (Å^3)	a/c	b/c
CoAs	0·0001	5·2857 (6)	5·8675 (6)	3·4883 (7)	108·19	1·5148 (5)	1·6816 (5)
	2·80 (5)	5·2675 (2)	5·815 (1)	3·4623 (1)	106·05	1·5214 (5)	1·6795 (5)
	3·70 (5)	5·2631 (3)	5·801 (1)	3·4569 (1)	105·54	1·5225 (5)	1·6781 (5)
	4·90 (5)	5·2575 (7)	5·7782 (6)	3·4453 (2)	104·67	1·5260 (5)	1·6771 (5)
FeAs	0·0001	5·4401 (5)	6·0259 (5)	3·3712 (4)	110·87	1·6137 (5)	1·7875 (5)
	2·25 (5)	5·4240 (6)	5·9948 (3)	3·3386 (2)	108·56	1·6246 (5)	1·7956 (5)
	4·36 (5)	5·411 (3)	5·9671 (8)	3·3122 (4)	106·93	1·634 (2)	1·8016 (5)
	6·10 (5)	5·403 (2)	5·9488 (8)	3·2902 (4)	105·74	1·642 (1)	1·8080 (5)
	8·3 (3)	5·390 (3)	5·928 (2)	3·2662 (6)	104·36	1·650 (1)	1·815 (1)

both models shows very little structural difference. Therefore, for both CoAs and FeAs, *Pnam* is considered to be the correct space group, and all refinements at high pressure were carried out in *Pnam*.

MnP-*type structure*

The MnP-type structure (Fig. 1*a*) is commonly a low-temperature polymorph of the NiAs-type structure (Fig. 1*b*) as seen in FeS (King & Prewitt, 1982), CrAs and CoAs (Selte & Kjekshus, 1973*b*). It is related by displacements of transition-metal atoms perpendicular to the NiAs c axis, and by nonmetal displacements along the c axis. In moving the metal atom from the center of the octahedral site, the distortion creates two closer and two further metal–metal contacts in the basal plane, and metal atoms form zigzag chains both parallel and perpendicular to the c axis. In addition, the six previously equivalent M–X contacts of the NiAs-type structure become four different distances in the MnP-type structure. Two of these four have mirror equivalents, whereas the other two are in the mirror plane. The number of different bonds and their multiplicity is designated by the shorthand notation (2+2+1+1). The M–M face-sharing contacts along the pseudohexagonal a-axis direction, although forming kinked chains, remain equivalent. The X–X contacts (considered nonbonding), which form the framework of the structure, degenerate from two sixfold (6+6) equivalent sets, to five sets. Four of these are twofold equivalent, and one is fourfold equivalent (2+2+2+2+4). The longest of these X–X contacts is a twofold set which forms the octahedral edges through which the shortest edge-sharing M–M interactions occur. The resultant orthorhombic symmetry has a unit cell which corresponds to an orthohexagonal setting of the NiAs structure, with space group *Pnam* [No. 62, *Pnma* in *International Tables for X-ray Crystallography* (1952) where $b_{nam} = c_{nma}$ and $c_{nam} = b_{nma}$] with four formula units per unit cell. Occupation of special position 4(*c*), with site symmetry *m*, constrains all atoms to lie within the mirror plane.

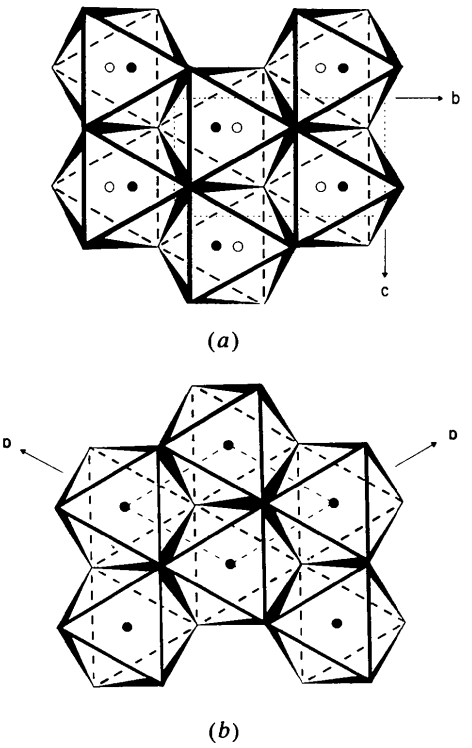

(*a*)

(*b*)

Fig. 1. A comparison of (*a*) the MnP-type structure and (*b*) the NiAs-type structure. In both figures blackened circles represent metal atoms in the plane shown, whereas empty circles represent those in the planes above and below. Unit cells are outlined in light dashed line.

High-pressure studies

Preliminary high-pressure studies of crystals, enclosed within a Merrill & Bassett diamond-anvil cell, were conducted using precession photography. Because the cell restricts the volume of reciprocal space available for investigation, crystals were loaded in such a manner to allow study of a particular section. In the case of CoAs and FeAs, the pseudohexagonal 0*kl* section was of particular interest.

Unit-cell-parameter data for both CoAs and FeAs show smooth variation with pressure (Table 3). The reluctance of a to decrease in both compounds reflects the resistance to shortening of the metal–metal face-sharing interactions along this direction. These distances are only 0·2–0·3 Å longer than they are in the pure metals. For both compounds, most of the volume decrease occurs through changes in b and c.

Table 4. *Summary of refinements in Pnam for* CoAs *and* FeAs

Compound	CoAs	CoAs	CoAs	CoAs	FeAs	FeAs	FeAs	FeAs	FeAs
Pressure (GPa)	0·0001	2·80 (5)	3·70 (5)	4·90 (5)	0·0001	2·25 (5)	4·36 (5)	6·10 (5)	8·3 (3)
Observed	991	370	374	531	528	550	542	538	538
Deleted*	10	55	64	77	0	80	102	92	84
Averaged set	283	90	89	151	276	125	119	120	131
R_w	0·054	0·039	0·040	0·046	0·030	0·035	0·037	0·046	0·050
R	0·049	0·037	0·041	0·047	0·023	0·032	0·038	0·037	0·043

* Includes absences collected and reflections with: contaminated background, bad agreement with symmetrical equivalents, angle > 42°.

Table 5. *Refined positional parameters for* CoAs *and* FeAs *in Pnam at room and high pressures*

Compound	CoAs	CoAs	CoAs	CoAs	FeAs	FeAs	FeAs	FeAs	FeAs
Pressure (GPa)	0·0001	2·80 (5)	3·70 (5)	4·90 (5)	0·0001	2·25 (5)	4·36 (5)	6·10 (5)	8·3 (3)
M[4(c)] x	0·0020 (2)	0·0023 (3)	0·0026 (3)	0·0032 (4)	0·0033 (1)	0·0032 (3)	0·0041 (5)	0·0029 (5)	0·0029 (5)
y	0·2002 (2)	0·1997 (6)	0·1987 (7)	0·1982 (2)	0·1993 (1)	0·1989 (2)	0·1985 (1)	0·1984 (3)	0·1980 (2)
z	1/4	1/4	1/4	1/4	1/4	1/4	1/4	1/4	1/4
As[4(c)] x	0·1996 (1)	0·1980 (1)	0·1974 (2)	0·1971 (3)	0·1992 (1)	0·1986 (2)	0·1979 (3)	0·1973 (4)	0·1969 (3)
y	0·5867 (1)	0·5862 (5)	0·5863 (5)	0·5870 (2)	0·5773 (1)	0·5766 (1)	0·5759 (1)	0·5752 (1)	0·5746 (1)
z	1/4	1/4	1/4	1/4	1/4	1/4	1/4	1/4	1/4

In some early work on MnP-type compounds, Pfisterer & Schubert (1950) divided this structure into two subgroups, distinguishing these on the basis of the b/c ratio. They suggested that higher valence-electron concentrations stabilize the structure with b/c lower than 1·732. Lower valence-electron concentrations stabilize the structure with b/c greater than 1·732. Rundqvist's (1962) studies of mixed phosphides, in which he finds $b/c = 1{\cdot}732$ at compositions $Co_{0{\cdot}6}Fe_{0{\cdot}4}P$, $Co_{0{\cdot}8}Mn_{0{\cdot}2}P$, and $Co_{0{\cdot}87}Cr_{0{\cdot}13}P$, all with d-electron concentration of 5·6, suggest structural control by d-electron concentration. With increasing pressure b/c decreases for CoAs, but increases for FeAs (Table 3). This contrasting pressure behavior may be related to differences in d-electron orbital or band occupation, as opposed to being simply a size phenomenom.

The unit-cell-volume data were used to determine the elastic constants, isothermal bulk modulus, and its pressure derivative (K_T and K'_T, respectively), by least-squares fitting of the unit-cell volumes to a third-order Birch–Murnaghan equation of state (Bass, Liebermann, Weidner & Finch, 1981). This gave K_T = 122·7 (6·1) GPa and $K'_T = 8{\cdot}8$ (3·3) for CoAs. For FeAs, $K_T = 118{\cdot}4$ (4·4) GPa and $K'_T = 7{\cdot}2$ (1·8). For comparison, the values obtained by King & Prewitt (1982) for FeS in the MnP-type structure are K_T = 34·8 (35) GPa and $K'_T = 5$ (2). Thus, FeAs and CoAs are less compressible than FeS. Owing to the greater electronegativity difference of Fe and S compared with that of Fe and As, and Co and As, the greater size difference should occur for Fe and S. Whether size differences, electronic factors, or both, explain the compressibilities is not clear because these factors are closely correlated.

For CoAs, data were collected and the structure refined (Tables 4 and 5) at three hydrostatic pressures; 2·80 (5), 3·70 (5) and 4·90 (5) GPa. the first two sets were collected on a small (0·06 × 0·12 × 0·15 mm) crystal which subsequently cracked at higher pressures. Another small (0·03 × 0·09 × 0·10 mm) crystal was used for data collection at 4·90 (5) GPa. This last crystal had been ground to a plate. Although data were not collected at pressures above 5 GPa, the study was continued at higher pressures using precession photography. A photograph taken at about 7·7 GPa showed significant change. The previously sharp zones and diffraction spots were diffuse and split. A similar effect was reported by King (1979) for FeS at 7·3 GPa (Fig. 2*b*). At 7·7 GPa there was still ample room between the CoAs crystal and gasket walls, although the hole had been shrinking with increasing pressure. Thus, we believe hydrostatic pressure conditions were maintained through this point. The diffuseness and splitting of the pattern for CoAs remained at pressures up to 9·7 GPa (Fig. 2*a*). Because the gasket wall was then touching the crystal, the cell was unloaded. While the pressure was reduced reversibility was checked. The splitting and diffuseness remained at room pressure. The crystal was dislodged from the gasket and mounted on a standard goniometer pin. Because a precession photograph revealed the same diffuseness of diffraction spots, we believe that the gasket wall did not contribute any non-hydrostatic effects at the highest pressures.

All high-pressure data for FeAs were collected from the same crystal (0·03 × 0·08 × 0·11 mm). A complete check of the data for beryllium or diamond interference resulted in no more than five reflections rejected from any data set for these reasons. Data were collected at four hydrostatic pressures; 2·25 (5), 4·36 (5), 6·10 (5), and 8·3 (3) GPa.

Table 6 lists interatomic distances for FeAs and CoAs at room and high pressures, and also for FeS in the MnP-type structure at high pressure (King & Prewitt, 1982). The face-sharing M–M distance

Table 6. *Nearest-neighbor interatomic distances for* CoAs, FeAs *and* FeS *in Pnam*

Compound	CoAs	CoAs	CoAs	CoAs	FeAs	FeAs	FeAs	FeAs	FeAs	FeS*	FeS*
Pressure (GPa)	0·0001	2·80 (5)	3·70 (5)	4·90 (5)	0·0001	2·25 (5)	4·36 (5)	6·10 (5)	8·3 (3)	4·15 (5)	6·35 (5)
M–M (Å)											
Face sharing	2·707 (2)	2·698 (4)	2·698 (4)	2·696 (5)	2·788 (1)	2·780 (4)	2·774 (6)	2·771 (6)	2·765 (6)	2·903 (12)	2·881 (12)
Edge sharing	2·927 (2)	2·897 (7)	2·882 (8)	2·865 (2)	2·935 (1)	2·911 (2)	2·891 (1)	2·875 (4)	2·860 (2)	2·919 (10)	2·843 (10)
Edge sharing	3·489 (1)	3·462 (1)	3·457 (1)	3·445 (1)	3·371 (1)	3·339 (1)	3·312 (1)	3·290 (1)	3·266 (1)	3·348 (10)	3·313 (10)
Edge sharing	3·927 (2)	3·898 (9)	3·900 (10)	3·890 (3)	3·997 (2)	3·977 (3)	3·961 (2)	3·948 (5)	3·935 (3)	3·800 (13)	3·814 (13)
M–X (Å)	2·322 (1)	2·309 (5)	2·305 (6)	2·303 (3)	2·348 (1)	2·336 (3)	2·329 (4)	2·317 (4)	2·309 (4)	2·316 (11)	2·311 (11)
	2·444 (1)	2·434 (3)	2·430 (3)	2·421 (3)	2·449 (1)	2·437 (2)	2·424 (3)	2·422 (4)	2·412 (3)	2·397 (8)	2·350 (8)
	2·396 (1)	2·397 (4)	2·377 (4)	2·370 (2)	2·422 (1)	2·408 (2)	2·398 (2)	2·386 (3)	2·376 (2)	2·473 (8)	2·461 (8)
	2·497 (1)	2·472 (7)	2·471 (7)	2·467 (3)	2·515 (1)	2·500 (2)	2·484 (2)	2·477 (4)	2·465 (3)	2·475 (12)	2·463 (11)
X–X (Å)	2·922 (1)	2·890 (3)	2·882 (3)	2·877 (3)	2·900 (1)	2·876 (2)	2·855 (3)	2·837 (4)	2·821 (3)	3·169 (11)	3·114 (11)
	3·265 (1)	3·250 (4)	3·245 (5)	3·234 (4)	3·425 (1)	3·417 (2)	3·411 (3)	3·409 (5)	3·404 (3)	3·492 (14)	3·438 (13)
	3·489 (1)	3·462 (1)	3·457 (1)	3·445 (1)	3·371 (1)	3·339 (1)	3·312 (1)	3·290 (1)	3·266 (1)	3·348 (10)	3·313 (10)
	3·455 (1)	3·428 (6)	3·422 (6)	3·409 (3)	3·496 (1)	3·476 (1)	3·459 (2)	3·446 (2)	3·432 (2)	3·363 (12)	3·331 (12)
	3·764 (1)	3·758 (2)	3·760 (3)	3·758 (4)	3·797 (1)	3·784 (3)	3·775 (4)	3·769 (5)	3·758 (4)	3·701 (12)	3·695 (12)

* Calculated using data from King & Prewitt (1982).

decreases very little, particularly in CoAs, whereas the edge-sharing *M–M* distance decreases more significantly. Of all the As–As edge distances of the octahedron, the longest, through which the shortest edge-sharing *M–M* interaction occurs, decreases least. This reflects the apparent strength of this interaction. This occurrence is most pronounced for CoAs, in which the As–As distance drops initially and then levels off at higher pressure. With this edge unable to decrease any more, the distortion becomes even more anisotropic. Because this As–As distance can still shorten in FeAs at pressures up to at least 8·3 GPa, its inability to shorten in CoAs may be an important factor in causing a transition at about 7·7 GPa. The validity of this suggestion is further strengthened by the similar changes of the interatomic distances of FeS in the MnP-type structure at high pressure. The longest S–S edge distance decreases barely, while all other S–S edge distances decrease more significantly. Also note that the Fe–Fe edge-sharing distance becomes shorter than the Fe–Fe face-sharing distance.

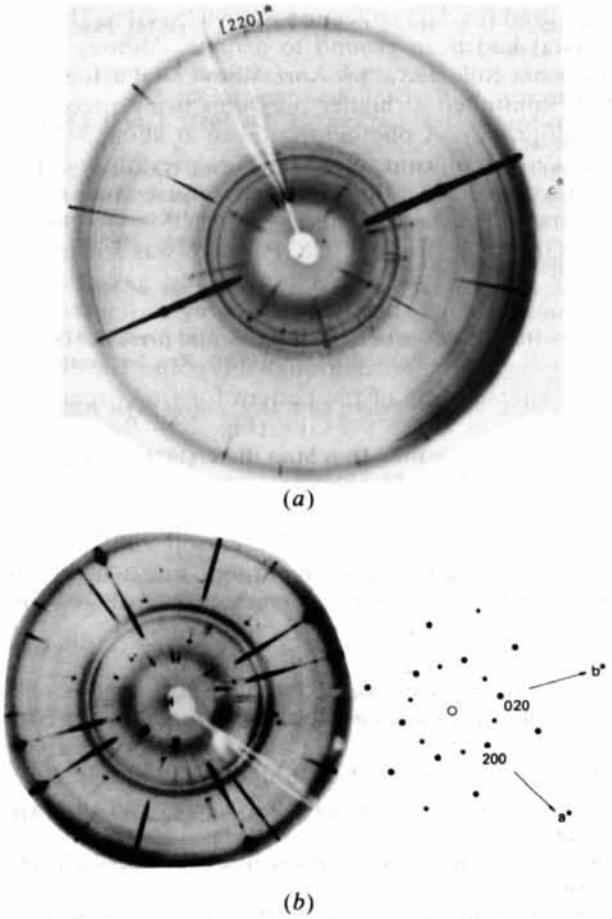

Fig. 2. High-pressure precession photographs of (*a*) CoAs at 9·8 GPa and (*b*) FeS (h.p.p.) at 7·3 GPa (photo from King, 1979). CoAs is not quite aligned with [220]* and *c** zones of an MnP-type cell. FeS is indexed with an NiAs-type cell.

Table 7. *Displacements* (Å) *of metal* (*M*) *and nonmetal* (*X*) *atoms from their positions in an* NiAs *unit cell for* FeS, CoAs *and* FeAs *in an* MnP-*type structure*

	Pressure (GPa)	Displacement(Å) *M*	*X*
FeS*	4·15 (5)	0·255	0·160
	6·35 (5)	0·282	0·170
CoAs	0·0001	0·292	0·266
	2·80 (5)	0·292	0·274
	3·70 (5)	0·297	0·277
	4·90 (5)	0·299	0·278
FeAs	0·0001	0·306	0·276
	2·25 (5)	0·306	0·279
	4·36 (5)	0·307	0·282
	6·10 (5)	0·307	0·285
	8·3 (3)	0·308	0·286

* From King & Prewitt (1982).

For FeS at high pressure, King & Prewitt (1982) calculated the displacements of the atoms from their positions in a NiAs structure. These displacements are also calculated for CoAs and FeAs, and are compared with those of FeS (Table 7). Note the constancy of the Fe displacement in FeAs, in contrast to the continually changing displacement of Co in CoAs,

and Fe in FeS. This suggests that any structural transitions are caused by eventual displacement of the metal atoms from their stable positions in the octahedra. These displacements may destabilize the metal–metal interactions that are important to the stability of these structures. This may be visualized as the arsenic octahedron collapsing around the metal atoms, and eventually interfering with the metal–metal interactions, particularly the edge-sharing ones. This interpretation is consistent with the constant decrease in magnetic ordering with increasing pressure for FeS in the MnP-type structure and then subsequent total breakdown of magnetic ordering when it transforms to FeS (h.p.p.) at 6·75 GPa (King, Virgo & Mao, 1978). Similar studies of CoAs and FeAs may add validity to this.

Summary

The results of this study are summarized as follows.

1. The crystal structures of both CoAs and FeAs are best described by space group *Pnam*. For CoAs this is consistent with its second-order transition to an NiAs-type structure at high temperature. For FeAs this is contrary to results of the Hamilton significance test, but this test is not a conclusive one. Insignificant changes in interatomic distances between models support the choice of *Pnam*.

2. Although the high-pressure study of CoAs and FeAs did not yield characterization of a phase transition, a transition in CoAs at about 7·8 GPa may occur. This belief is based on the splitting and diffuseness of diffraction spots, observed in a precession photograph, that are similar to that observed for FeS in its transition from an MnP-type structure to an uncharacterized high-pressure phase.

3. Changes in the interatomic distances reveal some interesting aspects of the MnP-type structure. Of the As–As distances, the longest, through which the shortest metal–metal edge-sharing interaction occurs, decreases least. In FeAs this distance still decreases at 8·3 GPa, whereas in CoAs it can no longer decrease at pressures greater than about 3·7 GPa. This effect is also seen in FeS before it undergoes a transition at 6·7 GPa. Therefore, if CoAs does undergo a transition at about 7·8 GPa, the inability of this distance to decrease any more may be an important factor in causing the transition.

4. The displacements of the atoms from their positions in an NiAs-type structure are also correlated with possible phase transitions in these structures. Both FeS and CoAs show significant metal-atom displacement, whereas FeAs shows little or none. The As displacements for all structures show continual displacement. These effects may be visualized as collapse of the As octahedron around the metal atom, and eventually interfering with the metal–metal edge-sharing interactions that are important to the stability of the structure.

We thank Mr Ken Baldwin, Dr John Parise and Dr Satoshi Sasaki for their valuable assistance with the experiments. This work was supported by National Science Foundation grant EAR 81-20950.

References

BARNETT, J. D., BLOCK, S. & PIERMARINI, G. J. (1973). *Rev. Sci. Instrum.* **44**, 1–9.

BASS, J. D., LIEBERMANN, R. C., WEIDNER, D. J. & FINCH, S. J. (1981). *Phys. Earth Planet. Inter.* **25**, 140–158.

BURNHAM, C. W. (1966). *Am. Mineral.* **51**, 159–167.

CROMER, D. T. & WABER, J. T. (1974). In *International Tables for X-ray Crystallography*, Vol. IV, pp. 71–147. Birmingham: Kynoch Press.

FINGER, L. W., HADIDIACOS, C. G. & OHASHI, Y. (1973). *Carnegie Inst. Washington Yearb.* **72**, 694–699.

FINGER, L. W. & KING, H. (1978). *Am. Mineral.* **63**, 337–342.

FINGER, L. W. & PRINCE, E. (1975). *Natl Bur. Stand. (US) Tech. Note*, pp. 854–981.

FRANZEN, H. F., HAAS, C. & JELLINEK, F. (1974). *Phys. Rev. B*, **10**, 1248–1250.

FYLKING, K. E. (1935). *Ark. Kemi, Mineral. Geol.* **B11**, No. 48.

HAMILTON, W. C. (1965). *Acta Cryst.* **18**, 502–510

HEYDING, R. D. & CALVERT, L. D. (1957). *Can. J. Chem.* **35**, 449–457.

HUBBELL, J. H., MCMASTER, W. H., DEL GRANDE, N. K. & MALLETT, J. H. (1974). *International Tables for X-ray Crystallography*, Vol. IV, pp. 47–70. Birmingham: Kynoch Press.

International Tables for X-ray Crystallography (1952). Vol. I. Birmingham: Kynoch Press.

KING, H. E. JR (1979). PhD Thesis, State Univ. of New York at Stony Brook.

KING, H. E. JR & FINGER, L. W. (1979). *J. Appl. Cryst.* **12**, 374–378.

KING, H. E. JR & PREWITT, C. T. (1980). *Rev. Sci. Instrum.* **51**, 1037–1039.

KING, H. E. JR & PREWITT, C. T. (1982). *Acta Cryst.* **B38**, 1877–1887.

KING, H. E. JR, VIRGO, D. & MAO, H. K. (1978). *Carnegie Inst. Washington Yearb.* **77**, 830–835.

MCCAMMON, C. A. (1982). *J. Phys. Chem. Solids*, **43**, 431–437.

MERRILL, L. & BASSETT, W. A. (1974). *Rev. Sci. Intrum.* **45**, 290–294.

PFISTERER, H. & SCHUBERT, K. Z. (1950). *Z. Metallkd.* **41**, 358.

PIERMARINI, G. J., BLOCK, S. & BARNETT, J. D. (1973). *J. Appl. Phys.* **44**, 5377–5382.

PIERMARINI, G. J., BLOCK, S., BARNETT, J. D. & FORMAN, R. A. (1975). *J. Appl. Phys.* **46**, 2774–2780.

RUNDQVIST, S. (1962). *Acta Chem. Scand.* **16**, 287–292.

SELTE, K. & KJEKSHUS, A. (1969). *Acta Chem. Scand.* **23**, 2047–2054.

SELTE, K. & KJEKSHUS, A. (1971). *Acta Chem. Scand.* **25**, 3277–3284.

SELTE, K. & KJEKSHUS, A. (1973*a*). *Acta Chem. Scand.* **27**, 1448–1449.

SELTE, K. & KJEKSHUS, A. (1973*b*). *Acta Chem. Scand.* **27**, 3195–3206.

SELTE, K., KJEKSHUS, A. & ANDRESEN, A. F. (1972). *Acta Chem. Scand.* **26**, 3101–3113.